A new *in vitro* assay measuring direct interaction of nonsense suppressors with the eukaryotic protein synthesis machinery

Martin Y. Ng[1], Haibo Zhang[1¥], Amy Weil[1†], Vijay Singh[2], Ryan Jamiolkowski[2], Alireza Baradaran-Heravi[3], Michel Roberge[3], Allan Jacobson[4], Westley Friesen[5], Ellen Welch[5], Yale E. Goldman[2], and Barry S. Cooperman[1*]

[1]Department of Chemistry, University of Pennsylvania, Philadelphia, PA 19104

[2]Department of Physiology, Perelman School of Medicine, University of Pennsylvania, Philadelphia, PA 19104

[3]Department of Biochemistry and Molecular Biology, University of British Columbia, Vancouver, BC, Canada V6T 1Z3

[4]Department of Microbiology and Physiological Systems, University of Massachusetts Medical School, Worcester, MA 01655

[5] PTC Therapeutics, 100 Corporate Court, South Plainfield, NJ 07080

* To whom to address inquiries

[¥] Present address: Spark Therapeutics, 3737 Market Street, Philadelphia, PA, 19104

[†] Present address: AdMed, Inc., 122 Union Square Drive, New Hope, PA, 18938

Abstract

Nonsense suppressors (NonSups) treat premature termination codon (PTC) disorders by inducing the selection of near cognate tRNAs at the PTC position, allowing readthrough of the PTC and production of full-length protein. Studies of NonSup-induced readthrough of eukaryotic PTCs have been carried out using animals, cells or crude cell extracts. In these studies, NonSups can promote readthrough directly, by binding to components of the protein synthesis machinery, or indirectly, by inhibiting nonsense-mediated mRNA decay or by other mechanisms. Here we utilize a highly-purified *in vitro* system (Zhang et al., 2016. *eLife* **5**: e13429) to measure exclusively direct NonSup-induced readthrough. Of 17 previously identified NonSups, 13 display direct effects, apparently via at least two different mechanisms. We can monitor such direct effects by single molecule FRET (smFRET). Future smFRET experiments will permit elucidation of the mechanisms by which NonSups stimulate direct readthrough, aiding ongoing efforts to improve the clinical usefulness of NonSups.

34 **Introduction**

35 Premature termination codons (PTCs) arise as a consequence of nonsense mutations and
36 lead to the replacement of an amino acid codon in mRNA by one of three stop codons, UAA, UGA
37 or UAG (Brenner, *et al.*, 1965; Shalev and Baasov, 2014; Keeling, *et al.*, 2014), resulting in
38 inactive truncated protein products. Nonsense mutations constitute ~20% of transmitted or *de novo*
39 germline mutations (Salvatori, *et al.*, 2009; Goldmann, *et al.*, 2012; Stenson, *et al.*, 2017). Globally,
40 there are ~7000 genetically transmitted disorders in humans and ~11% of all human disease
41 mutations are nonsense mutations (Loudon, 2013). Clearly, millions of people worldwide would
42 benefit from effective therapies directed toward PTC suppression. Clinical trials have begun to
43 evaluate the treatment of PTC disorders with therapeutic agents called nonsense suppressors
44 (NonSups) (Peltz, *et al.*, 2013; McDonald, *et al.*, 2017; Zainal Abidin, *et al.*, 2017). NonSups
45 induce the selection of near cognate tRNAs at the PTC position, and insertion of the corresponding
46 amino acid into the nascent polypeptide, a process referred to as "readthrough", which restores the
47 production of full length functional proteins, albeit at levels considerably reduced from wild-type.
48 Even low rates of readthrough can improve clinical outcomes when essential proteins are
49 completely absent. Examples of such essential proteins include Cystic Fibrosis Transmembrane
50 Regulator (CFTR) (Brodlie, *et al.*, 2015), dystrophin, and the cancer tumor suppressors
51 adenomatous polyposis coli (APS) (Floquet, *et al.*, 2011; Zilberberg, *et al.*, 2010) protein and p53
52 (Miyaki, *et al.*, 2002; Floquet, *et al.*, 2011; Roy, *et al.*, 2016; Baradaran-Heravi, *et al.*, 2016).

53 *In vitro, ex vivo,* and *in vivo* experiments and clinical trials have identified a diverse
54 structural set of NonSups as candidates for PTC suppression therapy (Figure 1), including
55 aminoglycosides (Shalev and Baasov, 2014; Bidou, *et al.*, 2017; Oishi, *et al.*, 2015; Duscha, *et al.*,
56 2014; Floquet, *et al.*, 2012; Sangkuhl, *et al.*, 2004; Fuchshuber-Moraes, *et al.*, 2011; Cogan, *et al.*,

57 2014; Baradaran-Heravi, *et al.*, 2017), ataluren (Peltz, *et al.*, 2013; Roy, *et al.*, 2016; Welch, *et al.*,
58 2007) and ataluren-like molecules (Du, *et al.*, 2009; Du, *et al.*, 2013; Gómez-Grau, *et al.*, 2015)
59 and others (Zilberberg, *et al.*, 2010; Arakawa, *et al.*, 2003; Hamada, *et al.*, 2015; Caspi, *et al.*,
60 2016; Mutyam, *et al.*, 2016). To date, only one NonSup, ataluren (known commercially as
61 Translarna), has been approved in the EU for clinical use, but this approval is limited to treatment
62 of patients with nonsense-mediated Duchenne muscular dystrophy. The clinical utility of other
63 NonSups, such as aminoglycosides, is restricted, in part, by their toxic side effects. A critical
64 barrier to development of NonSups that are more clinically useful is the paucity of information
65 regarding the precise mechanisms by which these molecules stimulate readthrough. All prior
66 results measuring nonsense suppressor-induced readthrough (NSIRT) of eukaryotic PTCs have
67 been carried out using animals, intact cells or crude cell extracts. In such systems, NonSups can
68 promote readthrough directly, by binding to one or more of the components of the protein synthesis
69 machinery, or indirectly, either by inhibiting nonsense-mediated mRNA decay (NMD) (He and
70 Jacobson, 2015), or by modulating processes altering the cellular activity levels of protein
71 synthesis machinery components (Feng, *et al.*, 2014; Keeling, 2016). These assays thus measure a
72 quantity we define as TOTAL-NSIRT. This multiplicity of possible mechanisms of nonsense
73 suppression within TOTAL-NSIRT has complicated attempts to determine the precise
74 mechanisms of action of specific NonSups and limited the use of rational design in identifying
75 new, more clinically useful NonSups.

76 Recently, we developed a highly purified, eukaryotic cell-free protein synthesis system
77 (Zhang, *et al.*, 2016) that we apply here to examine the direct effects of the NonSups on the protein
78 synthesis machinery, which we define as DIRECT-NSIRT. Our results allow us to distinguish
79 NonSups acting directly on the protein synthesis machinery from those that act indirectly and

80 suggest that NonSups having DIRECT-NSIRT effects can be divided into at least two distinctive
81 structural groups that induce nonsense suppression by different mechanisms. We also demonstrate
82 the potential of using single molecule fluorescence resonance energy transfer (smFRET)
83 experiments to elucidate the details of such mechanisms.
84
85 **Materials and Methods**
86 Nonsense suppressors (Figure 1). The following NonSups were obtained from commercial sources:
87 gentamicin mixture and G418 (Sigma), nourseothricin sulfate, a mixture of streptothricins D and
88 F (Gold Biotechnology), doxorubicin (Fisher Scientific), escin and tylosin (Alfa Aesar),
89 azithromycin (APExBIO). Gentamicins B and B1 were prepared as described (Baradaran-Heravi,
90 *et al.*, 2017). PTC Therapeutics supplied the following NonSups: ataluren sodium salt, RTC13,
91 GJ071, GJ072, and gentamicin X2. Negamycin was a gift from Alexander Mankin, University of
92 Illinois at Chicago. NB84 and NB124 (Bidou, *et al.*, 2017), currently available as ELX-02 and
93 ELX-03, respectively, from Eloxx Pharmaceuticals (Waltham, MA), were gifts from Timor
94 Baasov (Technion, Haifa).
95
96 Ribosomes and factors. Shrimp (*A. salina*) ribosome subunits were prepared from dried frozen
97 commercial cysts as described (Zhang, *et al.*, 2016; Iwasaki and Kaziro, 1979) with slight
98 modifications. Shrimp cysts (Pentair Aquatic Ecosystems) (425 g) were ground open using a
99 blender in the presence of buffer M (30 mM HEPES-KOH, pH 7.5, 50 mM KCl, 10 mM $MgCl_2$,
100 8.5% mannitol, 0.5 mM EDTA, 2 mM DTT, 1 mM PMSF, 1:3000 RNasin (New England Biolabs)
101 (500 mL), and two Protease Inhibitor Complete minitablets (Roche). Cyst debris was removed by
102 two centrifugations at 30,000 x g for 15 min at 4°C. 80S ribosomes in the supernatant were

103 precipitated by adding 175 mL of 4.5% PEG 20k (Ben-Shem, *et al.*, 2011) and resuspended in 60
104 mL of dissociation buffer 1 (20 mM HEPES-KOH, pH 7.5, 500 mM KCl, 2 mM $MgCl_2$, 6.8%
105 sucrose 2 mM DTT, 1:1000 RNasin, 2 protease minitablets). Puromycin was added to a final
106 concentration of 2 mM, and the resulting solution was incubated on ice for 30 min, then at 37 °C
107 for 15 min. 40S and 60S subunits (approximately 6,000 A_{260} units) were then resolved by a 10-
108 30% hyperbolic sucrose gradient centrifugation for 16 h in a Beckman Ti15 zonal rotor at 376,000
109 x g in dissociation buffer 2 (20 mM HEPES, pH 7.5, 0.5 M KCl, 5 mM $MgCl_2$, 3 mM EDTA, 2
110 mM DTT) at 4 ^{o}C. Carrier 70S ribosomes were isolated from S30 of *E. coli* cells by three
111 consecutive ultracentrifugations through a 1.1 M sucrose cushion in a buffer of 20 mM Tris, pH
112 7.5, 500 mM NH_4Cl, 10 mM Mg Acetate, 0.5 mM EDTA, 3 mM 2-mercaptoethanol. Elongation
113 factors eEF2 (Jørgensen, *et al.*, 2002) and eEF1A (Thiele, *et al.*, 1985) were isolated from Baker's
114 yeast as described. Yeast 6xHis-tagged release factors (full-length eRF1 and amino acids 166-685
115 of eRF3) were expressed in *E. coli* and purified using a TALON cobalt resin. Both release factors
116 were a generous gift from Alper Celik (University of Massachusetts Medical School).
117
118 <u>tRNA and mRNA</u>. $tRNA^{Lys}$, $tRNA^{Val}$, $tRNA^{Gln}$, and $tRNA^{Met}$ were isolated from *E. coli* bulk tRNA
119 (Roche). $tRNA^{Arg}$, $tRNA^{Trp}$ and $tRNA^{Leu}$ were isolated from Baker's yeast bulk tRNA (Roche),
120 using hybridization with immobilized complementary oligoDNA as described previously
121 (Barhoom, *et al.*, 2013; Liu, *et al.*, 2014). Yeast $tRNA^{Phe}$ (Sigma) and all isoacceptor tRNAs
122 mentioned above where charged with their cognate amino acids as described (Pan, *et al.*, 2007;
123 Pan, *et al.*, 2009). CrPV-IRES (Zhang, *et al.*, 2016) was modified by Genscript, Inc to encode the
124 initial mRNA sequence UUCAAAGUGAGA<u>UGG</u>CUAAUG (denoted Trp-IRES). A point
125 mutation was introduced into Trp-IRES to convert the UGG codon for Trp into a UGA stop codon

126 (UUCAAAGUGAGAUGACUAAUG, denoted Stop-IRES). These two sequences were inserted
127 into pUC57-Kan plasmid and amplified in TOP 10 competent cells. Plasmids were extracted using
128 QIAGEN Plasmid Kits and linearized. Trp-IRES and STOP-IRES were produced by in-vitro
129 transcription.
130
131 POST4 and POST5 Complex Preparation. 80S-IRES complex was first formed by incubating 0.8
132 μM 40S, 1.1 μM 60S and 0.8 μM IRES in Buffer 4 (40 mM Tris-HCl pH 7.5, 80 mM NH_4Cl, 5
133 mM $Mg(OAc)_2$, 100 mM KOAc, 3 mM 2-mercaptoethanol) at 37 °C for 2 min. Post-translocation
134 complex with FKVR-$tRNA^{Arg}$ in the ribosomal P-site tRNA (POST4) was formed by incubating
135 0.4 μM 80S-IRES with 0.4 μM each of the first four aminoacylated tRNAs, 0.4 μM eEF1A, 1.0
136 μM eEF2, 1 mM GTP at 37 °C for 25 min in Buffer 4. POST4 was then purified by
137 ultracentrifugation in 1.1 M sucrose with Buffer 4 at 540,000 x g for 90 min at 4°C. POST4 pellet
138 was resuspended in Buffer 4. Post-translocation complex with FKVRQ-$tRNA^{Gln}$ in the ribosomal
139 P-site tRNA (POST5) was prepared in identical fashion, except that the first five aminoacylated
140 tRNAs were added prior to the 25 min incubation at 37 °C. POST-4 amd POST-5 complexes could
141 be prepared and stored in small aliquots at -80 ^{0}C for at least three months with no discernible loss
142 of activity.
143
144 *In vitro* tRNA-Quant and PEP-Quant Readthrough Assays. POST5 complex (0.02 μM) was mixed
145 with Trp-$tRNA^{Trp}$, Leu-$tRNA^{Leu}$, and [^{35}S]-Met-$tRNA^{Met}$ (0.08 μM each), elongation factors
146 eEF1A (0.08 μM), eEF-2 (1.0 μM) and release factors eRF1 (0.010 μM) and eRF3 (0.020 μM)
147 and incubated at 37 °C in Buffer 4 for 20 min, in the absence or presence of NonSups.

148 For the tRNA-Quant Assay, reaction mixture aliquots (40 μL) were quenched with 150 μL
149 of 0.5 M MES buffer (pH 6.0). Following addition of carrier 70S *E. coli* ribosomes (100 pmol, 3
150 μL of 33 μM 70S), all ribosomes were pelleted by ultracentrifugation through a 1.1 M sucrose
151 solution in Buffer 4 (350 μL) at 540,000 x g for 70 min at 4°C. The ribosome pellet was
152 resuspended in Buffer 4, and co-sedimenting FKVRQWL[^{35}S]M-tRNA^{Met} was determined.
153 For the Pep-Quant Assay, reaction mixture aliquots (80 μL) were quenched with 0.8 M
154 KOH (9 μL of 8M KOH) and the base-quenched samples were incubated at 37 ^{o}C for 1 h to
155 completely release octapeptide FKVRQWL[^{35}S]M from tRNA^{Met}. Acetic acid (9 μL) was then
156 added to lower the pH to 2.8. Samples were next lyophilized, suspended in water, and centrifuged
157 to remove particulates. The particulates contained no ^{35}S. The supernatant was analyzed by thin
158 layer electrophoresis (TLE) as previously described (Youngman*, et al.*, 2004), using the same
159 running buffer. The identity of FKVRQWLM was confirmed by the co-migration of the ^{35}S
160 radioactivity with authentic samples obtained from GenScript (Piscataway, NJ). The ^{35}S
161 radioactivity in the octapeptide band was used to determine the amount of octapeptide produced.
162 In both assays, the assay background was determined as ^{35}S either co-sedimenting (tRNA-
163 Quant) or comigrating (PEP-Quant) in the absence of added Trp-tRNA^{Trp}. These levels were 0.09
164 ± 0.01 (sd, n = 80) octapeptide/POST5 for the tRNA-Quant assay and 0.04 ± 0.01 (sd, n = 8)
165 octapeptide/POST5 for the PEP-Quant assay. Some NonSups are poorly soluble in water and were
166 added to reaction mixtures from concentrated solutions made up in either DMSO (RTC13, GJ071,
167 GJ072, azithromycin) or methanol (escin). The level of organic solvent in the assay medium was
168 ≤ 0.5%. For these NonSups the small amount of readthrough induced in the presence of added
169 Trp-tRNA^{Trp} by added organic solvent (Table S1) was additionally subtracted as background.
170 Readthrough levels presented in Figures 3 and S3 are all background subtracted. Although PEP-

171 Quant has a lower procedural background, it is time consuming to perform, and less precise than
172 tRNA-Quant. Both assays show a basal level of readthrough, in the absence of added NonSup, of
173 0.08 ± 0.02 (sd, n=40) octapeptide/POST5 above background, with some day-to-day variation.
174
175 smFRET experiments. Fluorescent ternary complexes (TCs) were prepared by incubating 1 μM
176 eEF-1A, 3 μM GTP, and 1 μM charged tRNAs labeled with either Cy3 or Cy5 (Chen*, et al.*, 2011)
177 at 37 °C for 15 min in Buffer 4. For experiments measuring only PRE6 complex formation, POST4
178 complex, containing FVKR-$tRNA^{Arg}$ in the P-site and formed from ribosomes programmed with
179 either Trp-IRES or Stop-IRES biotinylated at the 5' end (Chen*, et al.*, 2011), was incubated with
180 15 nM Gln-TC(Cy5), 1 μM eEF-2 and 2 mM GTP in buffer 4 for 5 min at room temperature. The
181 resulting POST5 complex was immobilized on a streptavidin/biotin-PEG coated glass surface
182 (Chen*, et al.*, 2011). After two minutes of incubation, unbound reaction components were washed
183 out of the channel and 15 nM Trp-TC(Cy3) was added, with or without a NonSup, into the channel
184 to make a PRE6 complex. Unbound Trp-TC(Cy3) was washed out of the channel with Buffer 4
185 containing a deoxygenation enzyme system of 100 μg/mL glucose oxidase, 3 mg/mL glucose, and
186 48 μg/mL catalase to minimize photobleaching. Cy3 and Cy5 fluorescence intensities were
187 collected with 100 ms time resolution using alternating laser excitation (ALEX) between 532 nm
188 and 640 nm lasers on an objective-type total internal reflection fluorescence microscope described
189 previously (Chen*, et al.*, 2011). For experiments measuring both PRE6 complex and POST6
190 complex formation, Trp-IRES-PRE6 complex was formed as described above and 1 μM eEF-2
191 was injected while recording the FRET between FVKRQW-$tRNA^{Trp}$(Cy3) and $tRNA^{Gln}$(Cy5).
192 Ataluren ^{19}F NMR Spectroscopy. Various concentrations of ataluren solutions (0.03, 0.1 and 2.0
193 mM) were prepared in buffer 4 with 10% D_2O. The ^{19}F NMR spectrum of each solution was

194 recorded on a Bruker DMX 360 MHz NMR spectrometer with a 5 mm Quattro Nucleus Probe.
195 Data were analyzed with mNova software.
196
197 **Results**
198 The *in vitro* ribosomal readthrough assay. Structural studies (Fernández, *et al.*, 2014; Koh, *et al.*,
199 2014; Muhs, *et al.*, 2015; Murray, *et al.*, 2016; Abeyrathne, *et al.*, 2016) have shown that, prior to
200 polypeptide chain elongation, the cricket paralysis virus (CrPV) IRES structure occupies all three
201 tRNA binding sites (E, P, and A) on the 80S ribosome. We have recently demonstrated that the
202 first two cycles of peptide elongation proceed very slowly due to very low rates of pseudo-
203 translocation and translocation, but that, following translocation of tripeptidyl-tRNA, subsequent
204 elongation cycles proceed more rapidly (Zhang, *et al.*, 2016). Based on these results we
205 constructed an assay to directly monitor readthrough of the sixth codon, when the faster elongation
206 rate is well established. For this purpose, we prepared the two CrPv IRES coding sequences,
207 STOP-IRES and Trp-IRES (Figure 2). STOP-IRES contains the stop codon UGA at position 6 and
208 has a peptide coding sequence designed to give a high amount of readthrough, based on previous
209 studies showing that readthrough at the UGA stop codon proceeds in higher yields than at either
210 the UAA and UAG stop codons (Dabrowski, *et al.*, 2015) and that such readthrough is further
211 increased by both a downstream CUA codon (encoding Leu) at positions +4 - +6 (Stiebler, *et al.*,
212 2014; Loughran, *et al.*, 2014) and an upstream AA sequence at positions -1 and -2 (Dabrowski, *et*
213 *al.*, 2015). In TRP-IRES UGA is replaced by UGG which is cognate to $tRNA^{Trp}$, the most efficient
214 natural tRNA suppressor of the UGA codon (Blanchet, *et al.*, 2014; Roy, *et al.*, 2015). Trp-IRES
215 encodes the octapeptide FKVRQWLM, which permits facile quantification of octapeptide
216 synthesis by ^{35}S-Met incorporation.

217 For the results reported below, we first prepared two POST5 translocation complexes, each
218 containing FKVRQ-tRNA^{Gln} in the P-site, using ribosomes programmed with either STOP-IRES
219 or TRP-IRES. We then used the tRNA-Quant assay, which is rapid and precise, to determine the
220 amount of FKVRQWLM-tRNA^{Met} formed on incubating each POST5 complex with a mixture of
221 Trp-tRNA^{Trp}, Leu-tRNA^{Leu}, [^{35}S]-Met-tRNA^{Met}, elongation factors eEF1A and eEF2 and release
222 factors eRF1 and eRF3. We verified the validity of the tRNA-Quant assay by demonstrating that
223 it gives results that are very similar to those obtained with the PEP-Quant assay (Figure S1), in
224 which, following base treatment, the amount of FKVRQWLM octapeptide is determined following
225 a TLE separation procedure (Zhang*, et al.*, 2016; Youngman*, et al.*, 2004).
226
227 Induction of readthrough by aminoglycosides (AGs). Results with the eight AGs examined are all
228 consistent with a single tight site of AG binding to the ribosome (Garreau de Loubresse*, et al.*,
229 2014) resulting in increased readthrough, with EC_{50}s falling in the range of 0.14 – 4 μM and
230 fractional readthrough efficiencies of Stop-IRES varying from 0.1 – 0.3 (Table 1), as compared
231 with an efficiency of 1.00 ± 0.02 (n = 24) for conversion of POST5 to POST8 complex with Trp-
232 IRES (Figure 3A, Table 1). These results are consistent with results on readthrough obtained in
233 intact cells showing a) G418, gentamicin B1 (Baradaran-Heravi*, et al.*, 2017), NB84, NB124
234 (Bidou*, et al.*, 2017) and gentamicin X2 (Friesen*, et al.*, 2018) to be much more effective than the
235 gentamicin mixture currently used as an approved antibiotic; b) gentamicin B1 to be much more
236 effective than gentamicin B, despite their differing by only a single methyl group (Figure 1)
237 (Baradaran-Heravi*, et al.*, 2017); c) gentamicin B1 to be more effective than streptothricin (Figure
238 S2C); d) NB84, NB124 (Bidou*, et al.*, 2017), and gentamicin X2 (Friesen*, et al.*, 2018), to have
239 similar potencies, measured by either EC_{50} or readthrough efficiency.

240 Induction of readthrough by ataluren-like compounds. The NonSups ataluren, GJ072, and RTC 13
241 share similar structures, containing a central aromatic heterocycle having two or three substituents,
242 at least one of which is aromatic (Figure 1). They also show similar S-shaped readthrough activity
243 saturation curves (Figure 3B), with EC_{50} values between 0.17 – 0.35 mM and plateau readthrough
244 efficiencies ranging from 0.10 – 0.16 (Table 1). These S-shaped curves yield Hill n values of ~ 4,
245 which suggest multi-site binding of ataluren-like NonSups to the protein synthesis machinery.
246 Formation of NonSup aggregates in solution that induce readthrough could also give rise to S-
247 shaped curves, but we consider this to be unlikely based on the constancy of the chemical shift and
248 line shape of ataluren's ^{19}F NMR peak over a concentration range of 0.03 – 2.0 mM (see
249 Supplementary Information).
250
251 Induction of readthrough by other NonSups. Two other reported NonSups, negamycin (Taguchi,
252 *et al.*, 2017) and doxorubicin (Mutyam, *et al.*, 2016) also display readthrough activity in the tRNA-
253 Quant assay (Figure 3B). The results with each fit a simple saturation curve. Both NonSups have
254 similar readthrough efficiencies (0.10 – 0.13) but a 50-fold difference in EC_{50} values, with
255 doxorubicin having the much lower value (Table 1). Several other compounds that have
256 readthrough activity in cellular assays, tylosin (Zilberberg, *et al.*, 2010), azithromycin (Caspi, *et*
257 *al.*, 2016), GJ071 (Du, *et al.*, 2013) and escin (Mutyam, *et al.*, 2016) showed little or no activity
258 in the tRNA-Quant assay in the concentration range 30 – 600 μM (Figure S3). In addition, escin
259 at high concentration inhibits both basal readthrough elongation and normal elongation, the latter
260 measured with Trp-IRES programmed ribosomes, with the effect on basal readthrough being much
261 more severe (Figure S4).
262

263 Single molecule assay of readthrough activity. Two fluorescent labeled tRNAs, when bound
264 simultaneously to a ribosome, at either the A- and P-sites in a pretranslocation complex, or the P-
265 and E-sites in a postranslocation complex, are close enough to generate a FRET signal (Chen*, et*
266 *al.*, 2011; Blanchard*, et al.*, 2004). We observed tRNA-tRNA FRET in the pretranslocation
267 complex (Trp-IRES-PRE6), formed by incubating the Cy5-labeled Trp-IRES-POST5 with Cy3-
268 labeled eEF1A.GTP.Trp-$tRNA^{Trp}$, and having $tRNA^{Gln}$(Cy5) in the P-site and FKVRQW-
269 $tRNA^{Trp}$(Cy3) in the A-site (Figure 4). Addition of eEF2.GTP converted Trp-IRES-PRE6 to a Trp-
270 IRES-POST6 complex, containing $tRNA^{Gln}$(Cy5) in the E-site and FKVRQW-$tRNA^{Trp}$(Cy3) in
271 the P-site, which is accompanied by an increase in Cy3:Cy5 FRET efficiency (Figure 4).
272 Repetition of this experiment with Stop-IRES-POST5 in the absence of eEF2 decreased the
273 number of pretranslocation complexes (STOP-IRES-PRE6) formed to 24% of that seen with Trp-
274 IRES (Figure 4). This value was increased in a dose-dependent manner by addition of either G418
275 or gentamicin B1 (Figure 4B), with relative potencies similar to those displayed in Table 1. G418
276 and gentamicin did not significantly affect formation of Trp-IRES-PRE6 from Trp-IRES-POST5
277 on addition of Cy3-labeled eEF1A.GTP.Trp-$tRNA^{Trp}$. The agreement between the ensemble and
278 single molecule assays demonstrates our ability to monitor NonSup-induced readthrough by
279 smFRET, which, in subsequent studies, will allow determination of the effects of NonSups on the
280 dynamics of the nascent peptide elongation cycle that commences with suppressor tRNA
281 recognition of a premature stop codon.
282
283 **Discussion**
284 Here we utilize a straightforward *in vitro* assay, tRNA-Quant, to measure direct nonsense
285 suppressor-induced readthrough (DIRECT-NSIRT) of a termination codon. In the tRNA-Quant
286 assay, the arrival of the UGA termination codon into the 40S subunit portion of the tRNA A-site

287 has two possible outcomes: termination of peptide synthesis via eRF1/eRF3-catayzed hydrolysis
288 of the P-site-bound FKVRQ-tRNA^{Gln} or readthrough via productive A-site binding of near-cognate
289 Trp-tRNA^{Trp} followed by productive binding of the cognate Leu-tRNA^{Leu} and Met- tRNA^{Met}
290 leading to FKVRQWLM-tRNA^{Met} formation. NonSups increase the readthrough percentage by
291 binding to one or more of the specific components of the protein synthesis apparatus present in the
292 assay. Our working hypothesis is that Direct-NSIRT is an important, perhaps dominant, part of
293 Total-NSIRT for NonSups showing parallel effects in tRNA-Quant and cellular assays, such as
294 those included in Table 1. In contrast, biological activities of NonSups showing strong
295 readthrough activity in cellular assays but little readthrough activity in tRNA-Quant (Figure S3),
296 are likely be dominated by indirect effects.

297 Our results suggest that aminoglycosides and ataluren-like compounds stimulate
298 readthrough by different mechanisms, AGs via binding to a single tight site on the ribosome and
299 ataluren-like compounds via weaker, multi-site binding. (Figures 3, S2; Table 1). The EC_{50} values
300 found in intact cells differ considerably from those measured by tRNA-Quant, being much higher
301 for AGs (Bidou*, et al.*, 2017; Baradaran-Heravi*, et al.*, 2017), and much lower for ataluren (Peltz*,*
302 *et al.*, 2013; Roy*, et al.*, 2016), RTC13 (Du*, et al.*, 2013) and GJ072 (Du*, et al.*, 2013). We attribute
303 these differences to the fact that positively charged aminoglycosides are taken up poorly into cells,
304 while uptake is favored for the hydrophobic ataluren-like molecules. Thus, vis-à-vis the culture
305 medium, intracellular concentration would be expected to be lower for AGs and higher for
306 ataluren, RTC13 and GJ072. Although the NonSups doxorubicin and negamycin have only modest
307 activities (Figure 3, Table 1) each of these compounds have potential interest for future
308 development. Doxorubicin has a relatively low EC_{50}, is clinically approved for use in cancer
309 chemotherapy, and is the subject of ongoing efforts to identify doxorubicin congeners having

310 lower toxicity than doxorubicin itself (Kizek, *et al.*, 2012; Edwardson, *et al.*, 2015). Negamycin
311 exhibits low acute toxicity and there are ongoing efforts to increase its readthrough activity via
312 structure – function studies (Taguchi, *et al.*, 2017).

313 A critical barrier to further development of NonSups that are clinically useful is the paucity
314 of information regarding the mechanisms by which they stimulate readthrough and misreading.
315 Aminoglycosides have well-characterized binding sites in both prokaryotic (Lin, *et al.*, 2018) and
316 eukaryotic ribosomes (Garreau de Loubresse, *et al.*, 2014), proximal to the small subunit decoding
317 center, that have been linked to their promotion of misreading. Similarly, the functionally
318 important prokaryotic ribosome binding site of negamycin has also been identified within a
319 conserved small subunit rRNA region that is proximal to the decoding center (Lin, *et al.*, 2018;
320 Spahn, *et al.*, 2001), and it is not unlikely that this site is also present in eukaryotic ribosomes.
321 However, nothing is known about the readthrough-inducing sites of action within the protein
322 synthesis apparatus of the ataluren-like NonSups (Figure 3B) or of doxorubicin. Indeed, it has even
323 been suggested that ataluren may not target the ribosome (Pibiri, *et al.*, 2015). Although
324 aminoglycosides have been the subject of detailed mechanism studies of their effects on
325 prokaryotic misreading (Liu, *et al.*, 2014; Pape, *et al.*, 2000; Gromadski and Rodnina, 2004;
326 Cochella, *et al.*, 2006; Tsai, *et al.*, 2013; Zhang, *et al.*, 2018), questions remain over their precise
327 modes of action, and detailed mechanistic studies on aminoglycoside stimulation of eukaryotic
328 readthrough and misreading are completely lacking. Virtually nothing is known about the
329 mechanisms of action of negamycin, doxorubicin, and the ataluren-like NonSups in stimulating
330 eukaryotic readthrough. Single molecule FRET is a method of choice for obtaining detailed
331 information about processive biochemical reaction mechanisms (Roy, *et al.*, 2008), particularly in
332 the study of protein synthesis (Perez and Gonzalez, 2011; Aitken, *et al.*, 2010; Wang, *et al.*, 2011;

333 Chen, *et al.*, 2013), because it permits determination of distributions, variations and fluctuations
334 among different ribosome conformational states and of complex multistep reaction trajectories.
335 Here we demonstrate the feasibility of using smFRET observations for detailed examination of
336 NonSup-stimulation of readthrough (Figure 4) and misreading, which, combined with other
337 mechanistic studies, should aid in achieving the understanding needed to improve the clinical
338 usefulness of NonSups.
339

340 **Acknowledgements**

341 We thank Drs. Alexander Mankin (University of Illinois at Chicago), Timor Baasov (Technion,
342 Haifa) and Alper Celik (University of Massachusetts Medical School) for reagents used in these
343 studies and Carla Zimmerman for technical assistance. This work was supported by research grants
344 to BSC from PTC Therapeutics and the Orphan Disease Center, University of Pennsylvania
345 (MDBR-17-108-CF1282X), to YEG (NIH GM118139), to MR (Michael Smith Foundation for
346 Health Research) and AJ (NIH GM27757 and GM122468).

347 References
348

349 1 Brenner, S., Stretton, A. O. W. & Kaplan, S. 1965. Genetic Code: The 'Nonsense'
350 Triplets for Chain Termination and their Suppression. *Nature* **206**: 994,
351 doi:10.1038/206994a0.

352 2 Shalev, M. & Baasov, T. 2014. When Proteins Start to Make Sense: Fine-tuning
353 Aminoglycosides for PTC Suppression Therapy. *MedChemComm* **5**: 1092-1105,
354 doi:10.1039/C4MD00081A.

355 3 Keeling, K. M., Xue, X., Gunn, G. & Bedwell, D. M. 2014. Therapeutics Based on Stop
356 Codon Readthrough. *Annu. Rev. Genom. Hum. Genet.* **15**: 371-394, doi:10.1146/annurev-
357 genom-091212-153527.

358 4 Salvatori, F. *et al.* 2009. Production of β-globin and adult hemoglobin following G418
359 treatment of erythroid precursor cells from homozygous β(0)39 thalassemia patients. *Am.*
360 *J. Hematol.* **84**: 720-728, doi:10.1002/ajh.21539.

361 5 Goldmann, T., Overlack, N., Möller, F., Belakhov, V., van Wyk, M., Baasov, T.,
362 Wolfrum, U. & Nagel-Wolfrum, K. 2012. A comparative evaluation of NB30, NB54 and
363 PTC124 in translational read-through efficacy for treatment of an USH1C nonsense
364 mutation. *EMBO Molecular Medicine* **4**: 1186-1199, doi:10.1002/emmm.201201438.

365 6 Stenson, P. D., Mort, M., Ball, E. V., Evans, K., Hayden, M., Heywood, S., Hussain, M.,
366 Phillips, A. D. & Cooper, D. N. 2017. The Human Gene Mutation Database: towards a
367 comprehensive repository of inherited mutation data for medical research, genetic
368 diagnosis and next-generation sequencing studies. *Hum. Genet.* **136**: 665-677,
369 doi:10.1007/s00439-017-1779-6.

370 7 Loudon, J. A. 2013. Repurposing amlexanox as a 'run the red light cure- all' with read-
371 through – a 'no-nonsense' approach to eersonalised medicine. *J. Bioanal. Biomed.* **5**:
372 079-096, doi:doi: 10.4172/1948-593X.1000086.

373 8 Peltz, S. W., Morsy, M., Welch, E. M. & Jacobson, A. 2013. Ataluren as an Agent for
374 Therapeutic Nonsense Suppression. *Annu. Rev. Med.* **64**: 407-425, doi:10.1146/annurev-
375 med-120611-144851.

376 9 McDonald, C. M. *et al.* 2017. Ataluren in patients with nonsense mutation Duchenne
377 muscular dystrophy (ACT DMD): a multicentre, randomised, double-blind, placebo-
378 controlled, phase 3 trial. *Lancet* **390**: 1489-1498, doi:10.1016/S0140-6736(17)31611-2.

379 10 Zainal Abidin, N., Haq, I. J., Gardner, A. I. & Brodlie, M. 2017. Ataluren in cystic
380 fibrosis: development, clinical studies and where are we now? *Expert Opin.*
381 *Pharmacother.* **18**: 1363-1371, doi:10.1080/14656566.2017.1359255.

382 11 Brodlie, M., Haq, I. J., Roberts, K. & Elborn, J. S. 2015. Targeted therapies to improve
383 CFTR function in cystic fibrosis. *Genome Med.* **7**: 101, doi:10.1186/s13073-015-0223-6.

384 12 Floquet, C., Rousset, J.-P. & Bidou, L. 2011. Readthrough of Premature Termination
385 Codons in the Adenomatous Polyposis Coli Gene Restores Its Biological Activity in
386 Human Cancer Cells. *PLoS One* **6**: e24125, doi:10.1371/journal.pone.0024125.

387 13 Zilberberg, A., Lahav, L. & Rosin-Arbesfeld, R. 2010. Restoration of APC gene function
388 in colorectal cancer cells by aminoglycoside- and macrolide-induced read-through of
389 premature termination codons. *Gut* **59**: 496-507, doi:10.1136/gut.2008.169805.

390 14 Miyaki, M., Iijima, T., Yasuno, M., Kita, Y., Hishima, T., Kuroki, T. & Mori, T. 2002.
391 High incidence of protein-truncating mutations of the p53 gene in liver metastases of
392 colorectal carcinomas. *Oncogene* **21**: 6689, doi:10.1038/sj.onc.1205887.

393 15 Floquet, C., Deforges, J., Rousset, J.-P. & Bidou, L. 2011. Rescue of non-sense mutated
394 p53 tumor suppressor gene by aminoglycosides. *Nucleic Acids Res.* **39**: 3350-3362,
395 doi:10.1093/nar/gkq1277.

396 16 Roy, B. *et al.* 2016. Ataluren stimulates ribosomal selection of near-cognate tRNAs to
397 promote nonsense suppression. *Proc. Natl. Acad. Sci. USA* **113**: 12508-12513,
398 doi:10.1073/pnas.1605336113.

399 17 Baradaran-Heravi, A. *et al.* 2016. Novel small molecules potentiate premature
400 termination codon readthrough by aminoglycosides. *Nucleic Acids Res.* **44**: 6583-6598,
401 doi:10.1093/nar/gkw638.

402 18 Bidou, L., Bugaud, O., Belakhov, V., Baasov, T. & Namy, O. 2017. Characterization of
403 new-generation aminoglycoside promoting premature termination codon readthrough in
404 cancer cells. *RNA Biol.* **14**: 378-388, doi:10.1080/15476286.2017.1285480.

405 19 Oishi, N. *et al.* 2015. XBP1 mitigates aminoglycoside-induced endoplasmic reticulum
406 stress and neuronal cell death. *Cell Death Dis.* **6**: e1763, doi:10.1038/cddis.2015.108.

407 20 Duscha, S. *et al.* 2014. Identification and Evaluation of Improved 4′-O-(Alkyl) 4,5-
408 Disubstituted 2-Deoxystreptamines as Next-Generation Aminoglycoside Antibiotics.
409 *mBio* **5**, doi:10.1128/mBio.01827-14.

410 21 Floquet, C., Hatin, I., Rousset, J.-P. & Bidou, L. 2012. Statistical Analysis of
411 Readthrough Levels for Nonsense Mutations in Mammalian Cells Reveals a Major
412 Determinant of Response to Gentamicin. *PLoS Genet.* **8**: e1002608,
413 doi:10.1371/journal.pgen.1002608.

414 22 Sangkuhl, K., Schulz, A., Römpler, H., Yun, J., Wess, J. & Schöneberg, T. 2004.
415 Aminoglycoside-mediated rescue of a disease-causing nonsense mutation in the V2
416 vasopressin receptor gene in vitro and in vivo. *Hum. Mol. Genet.* **13**: 893-903,
417 doi:10.1093/hmg/ddh105.

418 23 Fuchshuber-Moraes, M., Sampaio Carvalho, R., Rimmbach, C., Rosskopf, D., Alex
419 Carvalho, M. & Suarez-Kurtz, G. 2011. Aminoglycoside-induced suppression of

420 CYP2C19*3 premature stop codon. *Pharmacogenet. Genomics* **21**: 694-700,
421 doi:10.1097/FPC.0b013e328349daba.

422 24 Cogan, J., Weinstein, J., Wang, X., Hou, Y., Martin, S., South, A. P., Woodley, D. T. &
423 Chen, M. 2014. Aminoglycosides Restore Full-length Type VII Collagen by Overcoming
424 Premature Termination Codons: Therapeutic Implications for Dystrophic Epidermolysis
425 Bullosa. *Mol. Ther.* **22**: 1741-1752, doi:doi.org/10.1038/mt.2014.140.

426 25 Baradaran-Heravi, A. *et al.* 2017. Gentamicin B1 is a minor gentamicin component with
427 major nonsense mutation suppression activity. *Proc. Natl. Acad. Sci. USA* **114**: 3479-
428 3484, doi:10.1073/pnas.1620982114.

429 26 Welch, E. M. *et al.* 2007. PTC124 targets genetic disorders caused by nonsense
430 mutations. *Nature* **447**: 87, doi:10.1038/nature05756.

431 27 Du, L. *et al.* 2009. Nonaminoglycoside compounds induce readthrough of nonsense
432 mutations. *J. Exp. Med.* **206**: 2285-2297, doi:10.1084/jem.20081940.

433 28 Du, L. *et al.* 2013. A New Series of Small Molecular Weight Compounds Induce Read
434 Through of All Three Types of Nonsense Mutations in the ATM Gene. *Mol. Ther.* **21**:
435 1653-1660, doi:10.1038/mt.2013.150.

436 29 Gómez-Grau, M. *et al.* 2015. Evaluation of Aminoglycoside and Non-Aminoglycoside
437 Compounds for Stop-Codon Readthrough Therapy in Four Lysosomal Storage Diseases.
438 *PLoS One* **10**: e0135873, doi:10.1371/journal.pone.0135873.

439 30 Arakawa, M. *et al.* 2003. Negamycin Restores Dystrophin Expression in Skeletal and
440 Cardiac Muscles of *mdx* Mice. *J. Biochem.* **134**: 751-758, doi:10.1093/jb/mvg203.

441 31 Hamada, K., Taguchi, A., Kotake, M., Aita, S., Murakami, S., Takayama, K., Yakushiji,
442 F. & Hayashi, Y. 2015. Structure–Activity Relationship Studies of 3-epi-
443 Deoxynegamycin Derivatives as Potent Readthrough Drug Candidates. *ACS Med. Chem.*
444 *Lett.* **6**: 689-694, doi:10.1021/acsmedchemlett.5b00121.

445 32 Caspi, M. *et al.* 2016. A flow cytometry-based reporter assay identifies macrolide
446 antibiotics as nonsense mutation read-through agents. *J. Mol. Med.* **94**: 469-482,
447 doi:10.1007/s00109-015-1364-1.

448 33 Mutyam, V. *et al.* 2016. Discovery of Clinically Approved Agents That Promote
449 Suppression of Cystic Fibrosis Transmembrane Conductance Regulator Nonsense
450 Mutations. *Am. J. Respir. Crit. Care Med.* **194**: 1092-1103, doi:10.1164/rccm.201601-
451 0154OC.

452 34 He, F. & Jacobson, A. 2015. Nonsense-Mediated mRNA Decay: Degradation of
453 Defective Transcripts Is Only Part of the Story. *Annu. Rev. Genet.* **49**: 339-366,
454 doi:10.1146/annurev-genet-112414-054639.

455 35 Feng, T. *et al.* 2014. Optimal Translational Termination Requires C4 Lysyl
456 Hydroxylation of eRF1. *Mol. Cell* **53**: 645-654, doi:10.1016/j.molcel.2013.12.028.

457 36 Keeling, K. M. 2016. Nonsense Suppression as an Approach to Treat Lysosomal Storage
458 Diseases. *Diseases* **4**: 32, doi:10.3390/diseases4040032.

459 37 Zhang, H., Ng, M. Y., Chen, Y. & Cooperman, B. S. 2016. Kinetics of initiating
460 polypeptide elongation in an IRES-dependent system. *eLife* **5**: e13429,
461 doi:10.7554/eLife.13429.

462 38 Iwasaki, K. & Kaziro, Y. 1979. [60] Polypeptide chain elongation factors from pig liver.
463 Moldave, K. & L. Grossman, editors. *Methods Enzymol.* New York: Academic Press, **60**:
464 657-676.

465 39 Ben-Shem, A., Garreau de Loubresse, N., Melnikov, S., Jenner, L., Yusupova, G. &
466 Yusupov, M. 2011. The Structure of the Eukaryotic Ribosome at 3.0 Å Resolution.
467 *Science* **334**: 1524-1529, doi:10.1126/science.1212642.

468 40 Jørgensen, R., Carr-Schmid, A., Ortiz, P. A., Kinzy, T. G. & Andersen, G. R. 2002.
469 Purification and crystallization of the yeast elongation factor eEF2. *Acta Crystallogr.*
470 *Sect. D. Biol. Crystallogr.* **58**: 712-715, doi:doi:10.1107/S0907444902003001.

471 41 Thiele, D., Cottrelle, P., Iborra, F., Buhler, J. M., Sentenac, A. & Fromageot, P. 1985.
472 Elongation factor 1 alpha from Saccharomyces cerevisiae. Rapid large-scale purification
473 and molecular characterization. *J. Biol. Chem.* **260**: 3084-3089.

474 42 Barhoom, S., Farrell, I., Shai, B., Dahary, D., Cooperman, B. S., Smilansky, Z., Elroy-
475 Stein, O. & Ehrlich, M. 2013. Dicodon monitoring of protein synthesis (DiCoMPS)
476 reveals levels of synthesis of a viral protein in single cells. *Nucleic Acids Res.* **41**: e177-
477 e177, doi:10.1093/nar/gkt686.

478 43 Liu, J. *et al.* 2014. Monitoring Collagen Synthesis in Fibroblasts Using Fluorescently
479 Labeled tRNA Pairs. *J. Cell. Physiol.* **229**: 1121-1129, doi:doi:10.1002/jcp.24630.

480 44 Pan, D., Kirillov, S. V. & Cooperman, B. S. 2007. Kinetically Competent Intermediates
481 in the Translocation Step of Protein Synthesis. *Mol. Cell* **25**: 519-529,
482 doi:10.1016/j.molcel.2007.01.014.

483 45 Pan, D., Qin, H. & Cooperman, B. S. 2009. Synthesis and functional activity of tRNAs
484 labeled with fluorescent hydrazides in the D-loop. *RNA* **15**: 346-354,
485 doi:10.1261/rna.1257509.

486 46 Youngman, E. M., Brunelle, J. L., Kochaniak, A. B. & Green, R. 2004. The Active Site
487 of the Ribosome Is Composed of Two Layers of Conserved Nucleotides with Distinct
488 Roles in Peptide Bond Formation and Peptide Release. *Cell* **117**: 589-599,
489 doi:10.1016/S0092-8674(04)00411-8.

490 47 Chen, C. *et al.* 2011. Single-Molecule Fluorescence Measurements of Ribosomal
491 Translocation Dynamics. *Mol. Cell* **42**: 367-377, doi:10.1016/j.molcel.2011.03.024.

492 48 Fernández, Israel S., Bai, X.-C., Murshudov, G., Scheres, Sjors H. W. & Ramakrishnan,
493 V. 2014. Initiation of Translation by Cricket Paralysis Virus IRES Requires Its
494 Translocation in the Ribosome. *Cell* **157**: 823-831, doi:10.1016/j.cell.2014.04.015.

495 49 Koh, C. S., Brilot, A. F., Grigorieff, N. & Korostelev, A. A. 2014. Taura syndrome virus
496 IRES initiates translation by binding its tRNA-mRNA–like structural element in the
497 ribosomal decoding center. *Proc. Natl. Acad. Sci. USA* **111**: 9139-9144,
498 doi:10.1073/pnas.1406335111.

499 50 Muhs, M., Hilal, T., Mielke, T., Skabkin, Maxim A., Sanbonmatsu, Karissa Y., Pestova,
500 Tatyana V. & Spahn, Christian M. T. 2015. Cryo-EM of Ribosomal 80S Complexes with
501 Termination Factors Reveals the Translocated Cricket Paralysis Virus IRES. *Mol. Cell*
502 **57**: 422-432, doi:10.1016/j.molcel.2014.12.016.

503 51 Murray, J., Savva, C. G., Shin, B.-S., Dever, T. E., Ramakrishnan, V. & Fernández, I. S.
504 2016. Structural characterization of ribosome recruitment and translocation by type IV
505 IRES. *eLife* **5**: e13567, doi:10.7554/eLife.13567.

506 52 Abeyrathne, P. D., Koh, C. S., Grant, T., Grigorieff, N. & Korostelev, A. A. 2016.
507 Ensemble cryo-EM uncovers inchworm-like translocation of a viral IRES through the
508 ribosome. *eLife* **5**: e14874, doi:10.7554/eLife.14874.

509 53 Dabrowski, M., Bukowy-Bieryllo, Z. & Zietkiewicz, E. 2015. Translational readthrough
510 potential of natural termination codons in eucaryotes – The impact of RNA sequence.
511 *RNA Biol.* **12**: 950-958, doi:10.1080/15476286.2015.1068497.

512 54 Stiebler, A. C., Freitag, J., Schink, K. O., Stehlik, T., Tillmann, B. A. M., Ast, J. &
513 Bölker, M. 2014. Ribosomal Readthrough at a Short UGA Stop Codon Context Triggers
514 Dual Localization of Metabolic Enzymes in Fungi and Animals. *PLoS Genet.* **10**:
515 e1004685, doi:10.1371/journal.pgen.1004685.

516 55 Loughran, G., Chou, M.-Y., Ivanov, I. P., Jungreis, I., Kellis, M., Kiran, A. M., Baranov,
517 P. V. & Atkins, J. F. 2014. Evidence of efficient stop codon readthrough in four
518 mammalian genes. *Nucleic Acids Res.* **42**: 8928-8938, doi:10.1093/nar/gku608.

519 56 Blanchet, S., Cornu, D., Argentini, M. & Namy, O. 2014. New insights into the
520 incorporation of natural suppressor tRNAs at stop codons in Saccharomyces cerevisiae.
521 *Nucleic Acids Res.* **42**: 10061-10072, doi:10.1093/nar/gku663.

522 57 Roy, B., Leszyk, J. D., Mangus, D. A. & Jacobson, A. 2015. Nonsense suppression by
523 near-cognate tRNAs employs alternative base pairing at codon positions 1 and 3. *Proc.*
524 *Natl. Acad. Sci. USA* **112**: 3038-3043, doi:10.1073/pnas.1424127112.

525 58 Garreau de Loubresse, N., Prokhorova, I., Holtkamp, W., Rodnina, M. V., Yusupova, G.
526 & Yusupov, M. 2014. Structural basis for the inhibition of the eukaryotic ribosome.
527 *Nature* **513**: 517, doi:10.1038/nature13737.

528 59 Friesen, W. *et al.* 2018. The minor gentamicin complex component, X2, is a potent
529 premature stop codon readthrough molecule with therapeutic potential. *Submitted for*
530 *publication*.

531 60 Taguchi, A., Hamada, K. & Hayashi, Y. 2017. Chemotherapeutics overcoming nonsense
532 mutation-associated genetic diseases: medicinal chemistry of negamycin. *J. Antibiot.* **71**:
533 205, doi:10.1038/ja.2017.112.

534 61 Blanchard, S. C., Kim, H. D., Gonzalez, R. L., Puglisi, J. D. & Chu, S. 2004. tRNA
535 dynamics on the ribosome during translation. *Proc. Natl. Acad. Sci. U. S. A.* **101**: 12893-
536 12898, doi:10.1073/pnas.0403884101.

537 62 Kizek, R., Adam, V., Hrabeta, J., Eckschlager, T., Smutny, S., Burda, J. V., Frei, E. &
538 Stiborova, M. 2012. Anthracyclines and ellipticines as DNA-damaging anticancer drugs:
539 Recent advances. *Pharmacol. Ther.* **133**: 26-39, doi:10.1016/j.pharmthera.2011.07.006.

540 63 Edwardson, D. W., Narendrula, R., Chewchuk, S., Mispel-Beyer, K., Mapletoft, J. P. J. &
541 Parissenti, A. M. 2015. Role of Drug Metabolism in the Cytotoxicity and Clinical
542 Efficacy of Anthracyclines. *Curr. Drug Metab.* **16**: 412-426,
543 doi:10.2174/1389200216888150915112039.

544 64 Lin, J., Zhou, D., Steitz, T. A., Polikanov, Y. S. & Gagnon, M. G. 2018. Ribosome-
545 Targeting Antibiotics: Modes of Action, Mechanisms of Resistance, and Implications for
546 Drug Design. *Annu. Rev. Biochem* **87**: null, doi:10.1146/annurev-biochem-062917-
547 011942.

548 65 Spahn, C. M. T., Beckmann, R., Eswar, N., Penczek, P. A., Sali, A., Blobel, G. & Frank,
549 J. 2001. Structure of the 80S Ribosome from Saccharomyces cerevisiae—tRNA-
550 Ribosome and Subunit-Subunit Interactions. *Cell* **107**: 373-386, doi:10.1016/S0092-
551 8674(01)00539-6.

552 66 Pibiri, I., Lentini, L., Melfi, R., Gallucci, G., Pace, A., Spinello, A., Barone, G. & Di
553 Leonardo, A. 2015. Enhancement of premature stop codon readthrough in the CFTR gene
554 by Ataluren (PTC124) derivatives. *Eur. J. Med. Chem.* **101**: 236-244,
555 doi:10.1016/j.ejmech.2015.06.038.

556 67 Pape, T., Wintermeyer, W. & Rodnina, M. V. 2000. Conformational switch in the
557 decoding region of 16S rRNA during aminoacyl-tRNA selection on the ribosome. *Nat.*
558 *Struct. Biol.* **7**: 104, doi:10.1038/72364.

559 68 Gromadski, K. B. & Rodnina, M. V. 2004. Streptomycin interferes with conformational
560 coupling between codon recognition and GTPase activation on the ribosome. *Nat. Struct.*
561 *Mol. Biol.* **11**: 316, doi:10.1038/nsmb742.

562 69 Cochella, L., Brunelle, J. L. & Green, R. 2006. Mutational analysis reveals two
563 independent molecular requirements during transfer RNA selection on the ribosome. *Nat.*
564 *Struct. Mol. Biol.* **14**: 30, doi:10.1038/nsmb1183.

565 70 Tsai, A., Uemura, S., Johansson, M., Puglisi, Elisabetta V., Marshall, R. A., Aitken,
566 Colin E., Korlach, J., Ehrenberg, M. & Puglisi, Joseph D. 2013. The Impact of
567 Aminoglycosides on the Dynamics of Translation Elongation. *Cell Reports* **3**: 497-508,
568 doi:10.1016/j.celrep.2013.01.027.

569 71 Zhang, J., Pavlov, M. Y. & Ehrenberg, M. 2018. Accuracy of genetic code translation
570 and its orthogonal corruption by aminoglycosides and Mg^{2+} ions. *Nucleic Acids Res.* **46**:
571 1362-1374, doi:10.1093/nar/gkx1256.

572 72 Roy, R., Hohng, S. & Ha, T. 2008. A practical guide to single-molecule FRET. *Nat.*
573 *Methods* **5**: 507, doi:10.1038/nmeth.1208.

574 73 Perez, C. E. & Gonzalez, R. L. 2011. In vitro and in vivo single-molecule fluorescence
575 imaging of ribosome-catalyzed protein synthesis. *Curr. Opin. Chem. Biol.* **15**: 853-863,
576 doi:10.1016/j.cbpa.2011.11.002.

577 74 Aitken, C. E., Petrov, A. & Puglisi, J. D. 2010. Single Ribosome Dynamics and the
578 Mechanism of Translation. *Ann. Rev. Biophys.* **39**: 491-513,
579 doi:10.1146/annurev.biophys.093008.131427.

580 75 Wang, L., Wasserman, M. R., Feldman, M. B., Altman, R. B. & Blanchard, S. C. 2011.
581 Mechanistic insights into antibiotic action on the ribosome through single-molecule
582 fluorescence imaging. *Ann. N.Y. Acad. Sci.* **1241**: E1-E16, doi:doi:10.1111/j.1749-
583 6632.2012.06839.x.

584 76 Chen, C., Zhang, H., Broitman, S. L., Reiche, M., Farrell, I., Cooperman, B. S. &
585 Goldman, Y. E. 2013. Dynamics of translation by single ribosomes through mRNA
586 secondary structures. *Nat. Struct. Mol. Biol.* **20**: 582, doi:10.1038/nsmb.2544.
587

588

589

590

591

592

593 **TABLES**

Table 1. Non-Sup Induced Readthrough

NonSup	EC_{50} (μM)	Readthrough fraction[a]	Hill n
Aminoglycosides			
Gentamicin B1	0.14 ± 0.02	0.27 ± 0.01	-
Gentamicin X2	0.42 ± 0.08	0.31 ± 0.02	-
NB124	0.52 ± 0.05	0.21 ± 0.01	-
Gentamicin B	0.54 ± 0.15	0.081 ± 0.005	-
NB84	0.68 ± 0.06	0.19 ± 0.01	-
G418	0.99 ± 0.09	0.32 ± 0.01	-
Streptothricin	1.5 ± 0.3	0.26 ± 0.01	-
Commercial Gentamicin (mixture)	4.2 ± 0.6	0.29 ± 0.02	-
Ataluren-Like			
GJ072	98 ± 4	0.16 ± 0.01	4.2 ± 0.7
RTC13	270 ± 15	0.10 ± 0.01	3.1 ± 0.5
Ataluren	350 ± 20	0.15 ± 0.01	4.3 ± 0.8
Other			
Doxorubicin	9.8 ± 1.8	0.11 ± 0.01	-
Negamycin	490 ± 70	0.13 ± 0.01	-

[a]Plateau octapeptide formed/POST5

594

595

596

597

598

599

600

601

602

603

604

605 **FIGURES**

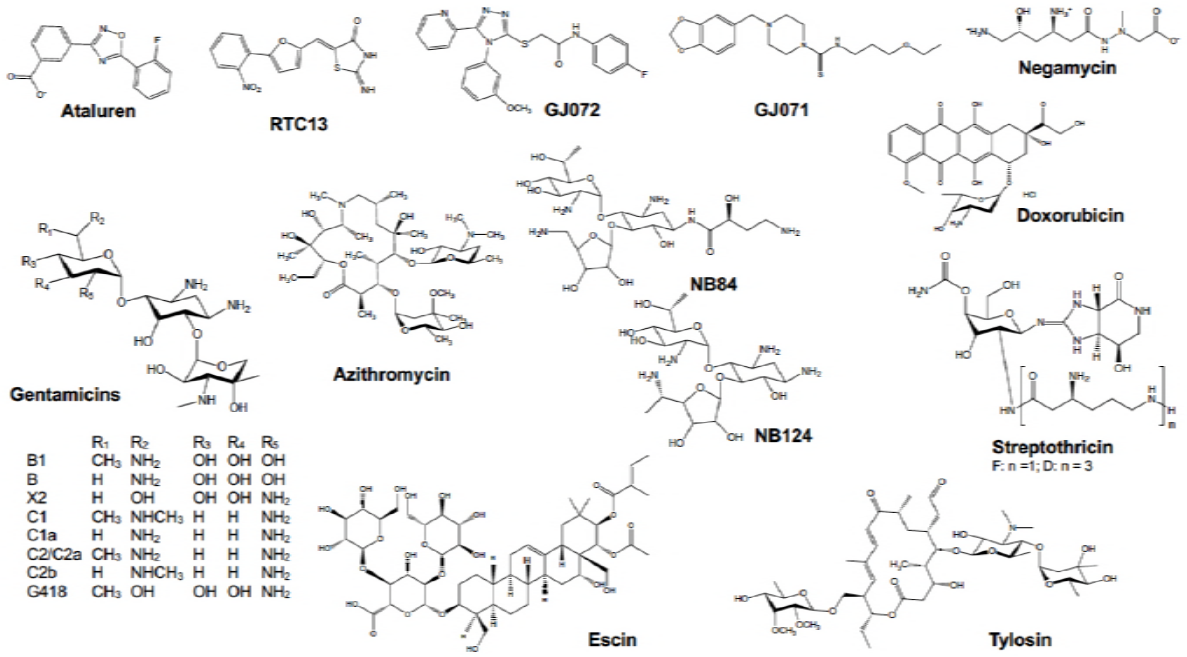

606

607 **Figure 1.** The structures of the nonsense suppressors (NonSups) studied in this work.

608

609

610

611

612

613

614

615

616

617

618

619

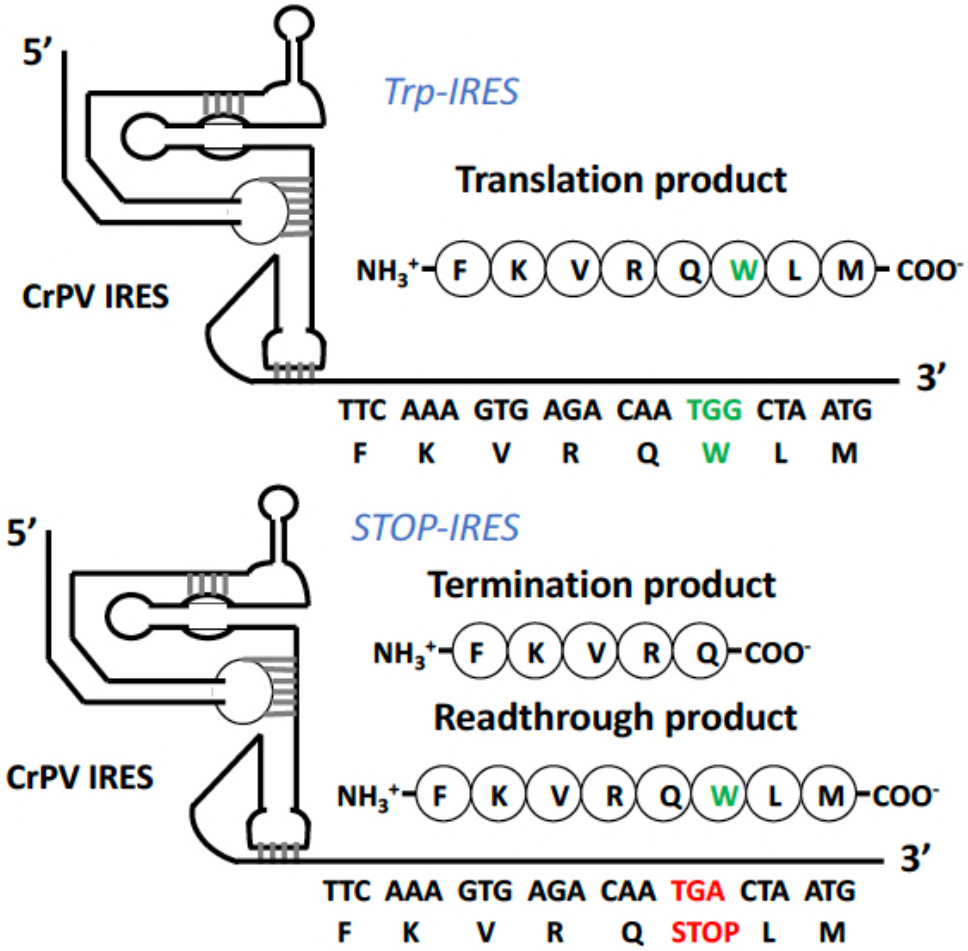

620

621 **Figure 2**. Coding sequences of Trp-IRES and Stop-IRES

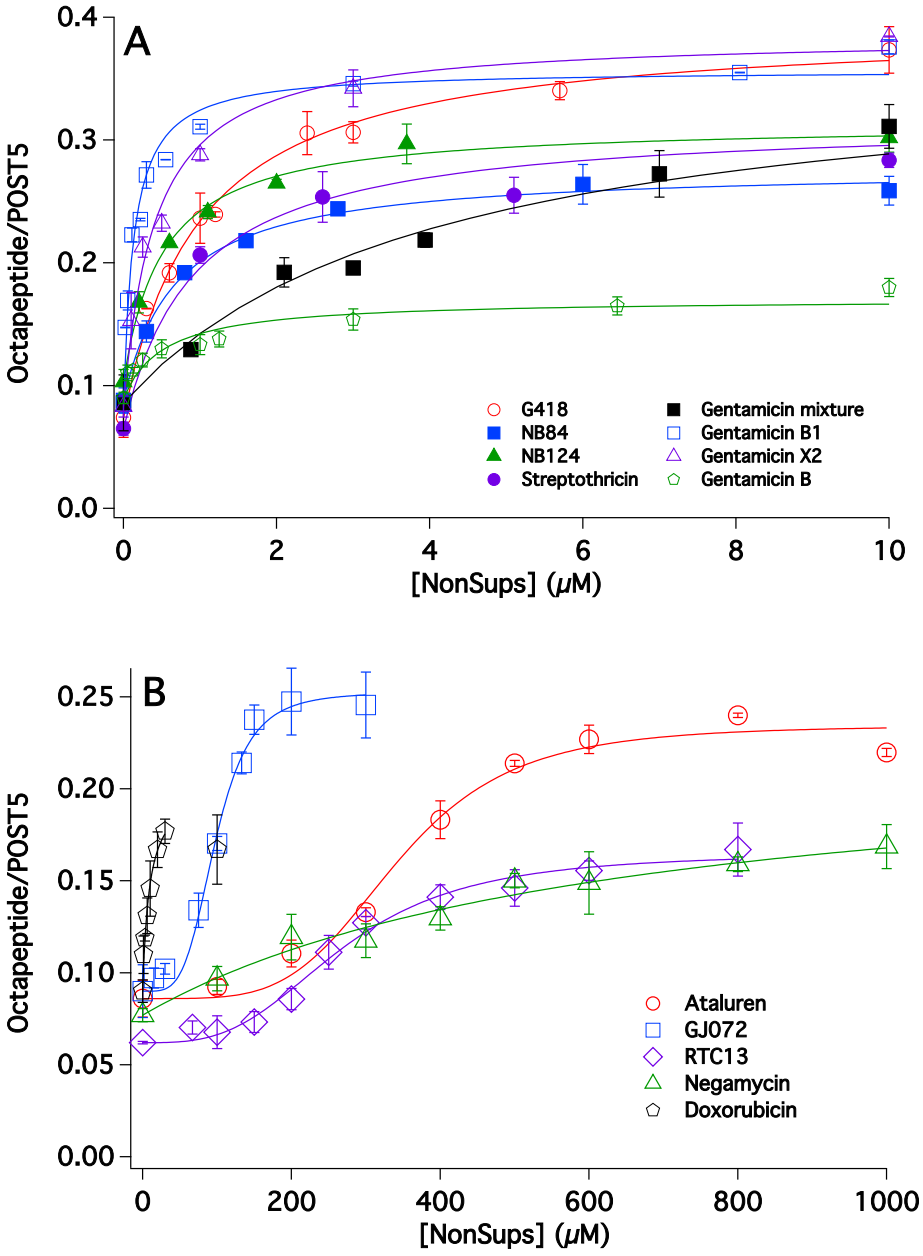

Figure 3. Readthrough as a function of nonsense suppressor concentration. A. Aminoglycosides. B. Ataluren-like NonSups and Others. The highest doxorubicin employed was 30 μM because higher concentrations led to significant ribosome and Met-tRNA^{Met} particle formation (Figure S5). None of the NonSups in Figure 3 showed appreciable inhibition of octapeptide formation from pentapeptide by ribosomes programmed with Trp-IRES at concentrations equal to twice their EC_{50} values.

630

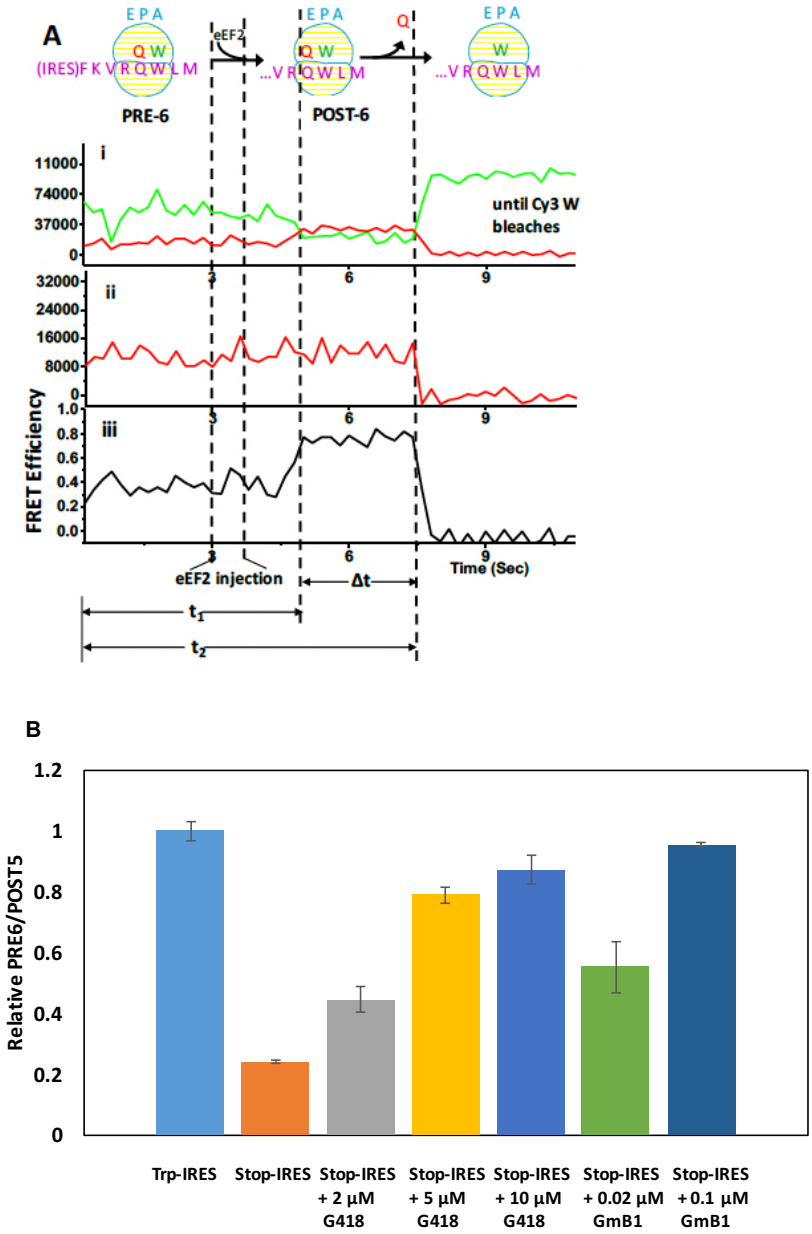

631

632 **Figure 4**. smFRET Experiments. A. eEF2-induced translocation of the 80S-Trp-IRES-PRE6

633 complex to form 80S-Trp-IRES-POST6 complex followed by release of $tRNA^{Gln}$. The Trp-IRES-

634 PRE6 complex contains $tRNA^{Gln}$(Cy5) in the P-site and FKVRQW-$tRNA^{Trp}$(Cy3) in the A-site.

635 The cartoon at top shows the state progression during translocation. i. Single molecule traces.

636 Green and red traces show $tRNA^{Trp}$(Cy3) emission and $tRNA^{Gln}$(Cy5) sensitized emission,

637 respectively, following eEF2 injection, excited at 532 nm. ii. ALEX intensity signal from direct
638 excitation of $tRNA^{Gln}$(Cy5) at 640 nm. iii. FRET efficiency between $tRNA^{Trp}$(Cy3) and
639 $tRNA^{Gln}$(Cy5) showing a transient increase following eEF2 on conversion of PRE6 complex to
640 POST6 complex. B. Dose-dependent effect of G418 and GmB1 (gentamicin B1) on PRE6
641 complex formation from 80S-Stop-IRES-POST5 complex as compared with PRE6 complex
642 formation from 80S-Trp-IRES-POST5 complex in the absence of either G418 or GmB1.
643

644 **SUPPLEMENTARY INFORMATION**

645 The tRNA-Quant and PEP-Quant assays give similar results (Figure S1).

646

647 Identification of streptothricin as a nonsense suppressor in yeast and human cells. An in-house
648 collection of 664 antimicrobial compounds was screened for suppression of two nonsense alleles
649 in *Saccharomyces cerevisiae* using a modification of a published procedure (Baradaran-Heravi*, et*
650 *al.*, 2016). Exponentially growing B0133-3B yeast cells harboring *met8-1* (TAG) and *trp5-48*
651 (TAA) nonsense alleles were seeded in 96-well plates at A_{600} = 0.01 in Synthetic Complete medium
652 containing 5 μM Met and 5 μM Trp. This strain is unable to grow in the presence of these low
653 concentrations of Met and Trp, unlike prototrophic strains. Antimicrobial compounds were added
654 individually to the wells using a Biorobotics TAS1 robot equipped with a 0.7 mm diameter 96-pin
655 tool, at a final concentration of ~15 μM. The plates were incubated at 30°C for 42 h and yeast
656 growth was determined by measuring A_{600}. Paromomycin was added at 10 μM to four wells as a
657 positive control. In this assay, yeast growth requires efficient suppression of both *met8-1* and *trp5-*
658 *48*. A single compound, streptothricin, enabled robust yeast growth (Figure S2A), with an EC_{50} of
659 5 μM (Figure S2B). Streptothricin was also assayed for nonsense suppression in human cells using
660 a previously described assay (Baradaran-Heravi *et al.,* 2016). Briefly, human breast carcinoma
661 HDQ-P1 cells homozygous for the *TP53* R213X (TGA) nonsense mutation were exposed to
662 different concentrations of streptothricin for 72 h and the production of full-length p53, the
663 readthrough product, and truncated p53 was determined by automated capillary electrophoresis
664 western analysis. Streptothricin showed weak readthrough activity, detectable at concentrations of
665 200 μM and above. By contrast, gentamicin B1 showed much higher levels of readthrough at lower
666 concentrations (Figure S2C).

667

668 Assay heterogeneity. The reaction mixtures used for the tRNA-Quant and Pep-Quant assays is
669 heterogeneous, with ribosomes derived from shrimp cysts or Hela cells, yeast elongation factors,
670 and yeast and *E. coli* charged tRNAs. However, such heterogeneity is not problematic. IRESs can
671 initiate translation on ribosomes from many eukaryotic organisms (Koh*, et al.*, 2014), including
672 shrimp (Cevallos and Sarnow, 2005), indicating that the molecular mechanism is not species-
673 specific. CrPV IRES can initiate translation on ribosomes from yeast (Thompson*, et al.*, 2001) to
674 human (Spahn*, et al.*, 2004). Furthermore, the structures of eukaryotic elongation factors are very
675 strongly conserved (Soares*, et al.*, 2009; Jørgensen*, et al.*, 2002), and charged tRNAs from one
676 species form fully functional complexes with both eEF1A and ribosomes from different ones
677 (Jackson*, et al.*, 2001; Ferguson*, et al.*, 2015).

678

679 Concentration dependence of Ataluren ^{19}F NMR chemical shift. A decrease in chemical shift of
680 an ^{19}F NMR peak provides an indication of molecular aggregation in solution (Iijima*, et al.*, 1999;
681 Ohta*, et al.*, 2003; Suzuki*, et al.*, 2013). We sought to determine whether aggregation was
682 responsible for the sigmoidal readthrough saturation curve for ataluren (Figure 3B) by examining
683 the chemical shift of its ^{19}F NMR peak at three concentrations, 0.03, 0.1 and 2.0 mM, that bracket
684 the range employed in the readthrough assay. We found that both the chemical shift (1.0 ppm
685 downfield from a KF standard) and the line shape of the ^{19}F NMR peak were identical at all three
686 concentrations, evidence that aggregation is unlikely to be the cause of the readthrough saturation
687 curve induced by ataluren.

688

689 NonSups having low activity in the tRNA-Quant assay (Figure S3)

690

691 Escin inhibition of octapeptide synthesis from POST-5 complexes. Escin concentrations ≥ 300 μM
692 inhibit octapeptide synthesis from POST5 complexes for ribosomes programmed with either Stop-
693 IRES (basal readthrough) or ribosomes programmed with Trp-IRES (normal octapeptide
694 synthesis), with inhibition being much more pronounced on basal readthrough (Figure S4). This
695 difference is not currently understood. One possibility under consideration is that inhibition arises
696 from a destabilization of peptidyl-tRNA binding to the A-site of a PRE6 complex, and that
697 such binding is weaker for ribosomes programmed with Stop-IRES vs. Trp-IRES.

698

699 Doxorubicin-induced particle formation by both tRNA and ribosomes. Doxorubicin
700 concentrations above 100 μM induced Met-tRNA^{Met} particle formation in accord with prior results
701 (Agudelo, *et al.*, 2016). High doxorubicin also induced particle formation by ribosome-IRES
702 complex (Figure S5). To determine the extent of particle formation, various concentrations of
703 doxorubicin were added to aliquots (250 μL) containing 0.1 μM 80S:IRES complex, 0.1 μM
704 [^{35}S]Met-tRNA^{Met}, 0.1 μM eEF1A and 1 mM GTP. The mixture was incubated at 37 °C for 20
705 min. Particles were removed by centrifugation at 17,000 X g for 25 min at 4 °C. The supernatant
706 was then layered on top of 350 μL Buffer 4 with 1.1 M sucrose and was ultracentrifuged at 540,000
707 x g for 70 min at 4°C to separate 80S-IRES from [^{35}S]Met-tRNA^{Met}. Virtually all of the A_{260} units
708 and [^{35}S] radioactivity (~98% in each case) of the low speed supernatant were found in the high
709 speed pellet and supernatant, respectively. Accordingly, measurements of A_{260} units and [^{35}S]
710 radioactivity in the low speed supernatant were used to determine the amounts of 80S-IRES and
711 [^{35}S]Met-tRNA^{Met} remaining in solution after doxorubicin-induced particle formation.

712

713
714 SUPPLEMENTARY REFERENCES
715

716 1 Baradaran-Heravi, A. *et al.* 2016. Novel small molecules potentiate premature
717 termination codon readthrough by aminoglycosides. *Nucleic Acids Res.* **44**: 6583-6598,
718 doi:10.1093/nar/gkw638.

719 2 Koh, C. S., Brilot, A. F., Grigorieff, N. & Korostelev, A. A. 2014. Taura syndrome virus
720 IRES initiates translation by binding its tRNA-mRNA–like structural element in the
721 ribosomal decoding center. *Proc. Natl. Acad. Sci. USA* **111**: 9139-9144,
722 doi:10.1073/pnas.1406335111.

723 3 Cevallos, R. C. & Sarnow, P. 2005. Factor-Independent Assembly of Elongation-
724 Competent Ribosomes by an Internal Ribosome Entry Site Located in an RNA Virus
725 That Infects Penaeid Shrimp. *J. Virol.* **79**: 677-683, doi:10.1128/jvi.79.2.677-683.2005.

726 4 Thompson, S. R., Gulyas, K. D. & Sarnow, P. 2001. Internal initiation in *Saccharomyces*
727 *cerevisiae* mediated by an initiator tRNA/eIF2-independent internal ribosome entry site
728 element. *Proc. Natl. Acad. Sci. USA* **98**: 12972-12977, doi:10.1073/pnas.241286698.

729 5 Spahn, C. M. T., Jan, E., Mulder, A., Grassucci, R. A., Sarnow, P. & Frank, J. 2004.
730 Cryo-EM Visualization of a Viral Internal Ribosome Entry Site Bound to Human
731 Ribosomes: The IRES Functions as an RNA-Based Translation Factor. *Cell* **118**: 465-
732 475, doi:10.1016/j.cell.2004.08.001.

733 6 Soares, D. C., Barlow, P. N., Newbery, H. J., Porteous, D. J. & Abbott, C. M. 2009.
734 Structural Models of Human eEF1A1 and eEF1A2 Reveal Two Distinct Surface Clusters
735 of Sequence Variation and Potential Differences in Phosphorylation. *PLoS One* **4**: e6315,
736 doi:10.1371/journal.pone.0006315.

737 7 Jørgensen, R., Carr-Schmid, A., Ortiz, P. A., Kinzy, T. G. & Andersen, G. R. 2002.
738 Purification and crystallization of the yeast elongation factor eEF2. *Acta Crystallogr.*
739 *Sect. D. Biol. Crystallogr.* **58**: 712-715, doi:doi:10.1107/S0907444902003001.

740 8 Jackson, R. J., Napthine, S. & Brierley, I. 2001. Development of a tRNA-dependent in
741 vitro translation system. *RNA* **7**: 765-773.

742 9 Ferguson, A. *et al.* 2015. Functional Dynamics within the Human Ribosome Regulate the
743 Rate of Active Protein Synthesis. *Mol. Cell* **60**: 475-486,
744 doi:10.1016/j.molcel.2015.09.013.

745 10 Iijima, H., Koyama, S., Fujio, K. & Uzu, Y. 1999. NMR Study of the Transformation of
746 Perfluorinated Surfactant Solutions. *Bull. Chem. Soc. Jpn.* **72**: 171-177,
747 doi:10.1246/bcsj.72.171.

748 11 Ohta, A., Murakami, R., Urata, A., Asakawa, T., Miyagishi, S. & Aratono, M. 2003.
749 Aggregation Behavior of Fluorooctanols in Hydrocarbon Solvents. *J. Phys. Chem. B* **107**:
750 11502-11509, doi:10.1021/jp035134o.

12 Suzuki, Y., Brender, J. R., Soper, M. T., Krishnamoorthy, J., Zhou, Y., Ruotolo, B. T., Kotov, N. A., Ramamoorthy, A. & Marsh, E. N. G. 2013. Resolution of Oligomeric Species during the Aggregation of Aβ(1-40) Using (19)F NMR. *Biochemistry* **52**: 1903-1912, doi:10.1021/bi400027y.

13 Agudelo, D., Bourassa, P., Bérubé, G. & Tajmir-Riahi, H. A. 2016. Review on the binding of anticancer drug doxorubicin with DNA and tRNA: Structural models and antitumor activity. *J. Photochem. Photobiol. B: Biol.* **158**: 274-279, doi:10.1016/j.jphotobiol.2016.02.032.

SUPPLEMENTARY TABLES

Table S1. DMSO and MeOH each induce added basal readthrough	
Volume % DMSO	Basal readthrough fraction[a] above –Trp-RNA^{Trp} background
0	0.078 ± 0.013
0.1	0.099 ± 0.004
0.33	0.12 ± 0.01
0.67	0.14 ± 0.01
1.0	0.15 ± 0.01
Volume % MeOH	
0	0.099 ± 0.012
0.17	0.10 ± 0.01
0.5	0.12 ± 0.01
1.0	0.14 ± 0.01
[a]normalized to octapeptide synthesis by Trp-IRES in the absence of either DMSO or MeOH	

817 **SUPPLEMENTARY FIGURES**

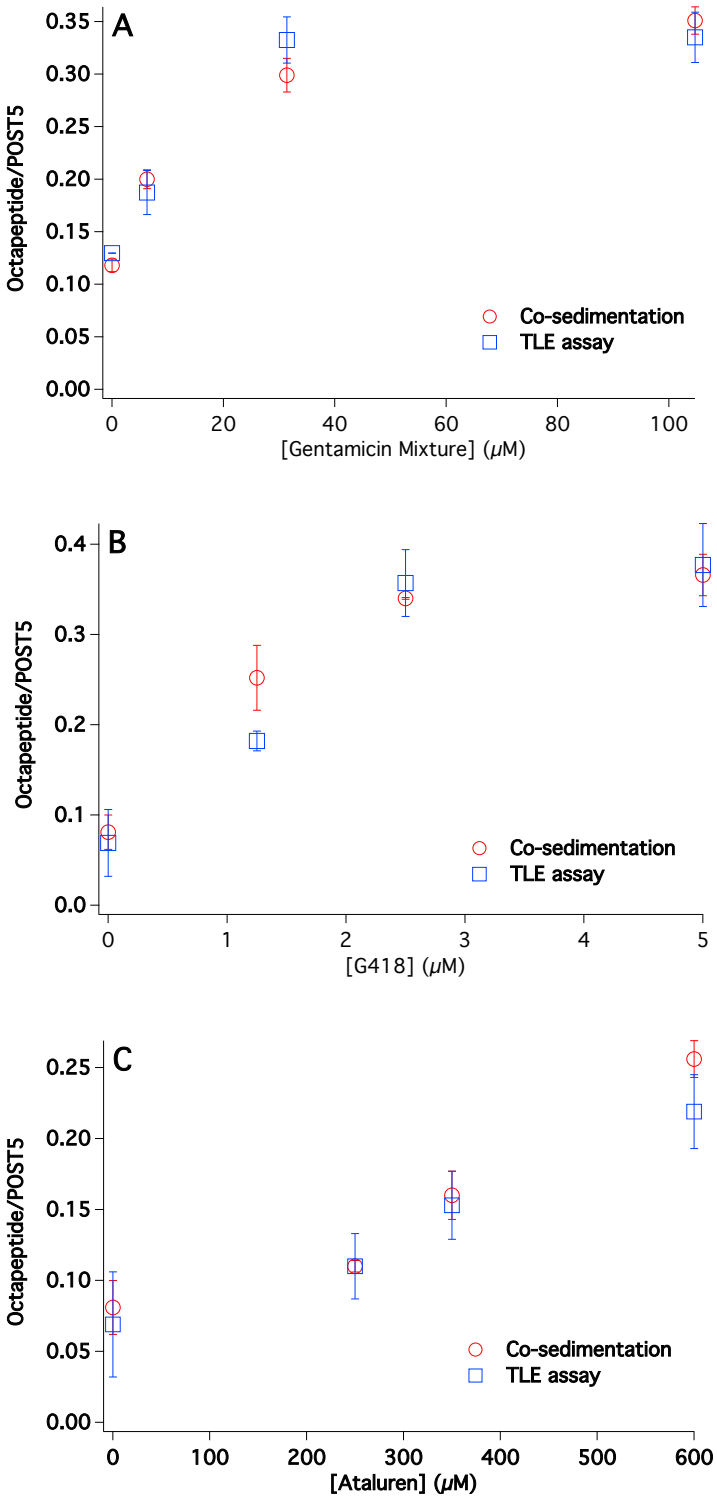

818

819

820

821 **Supplementary Figure 1**. tRNA-Quant vs. Pep-Quant

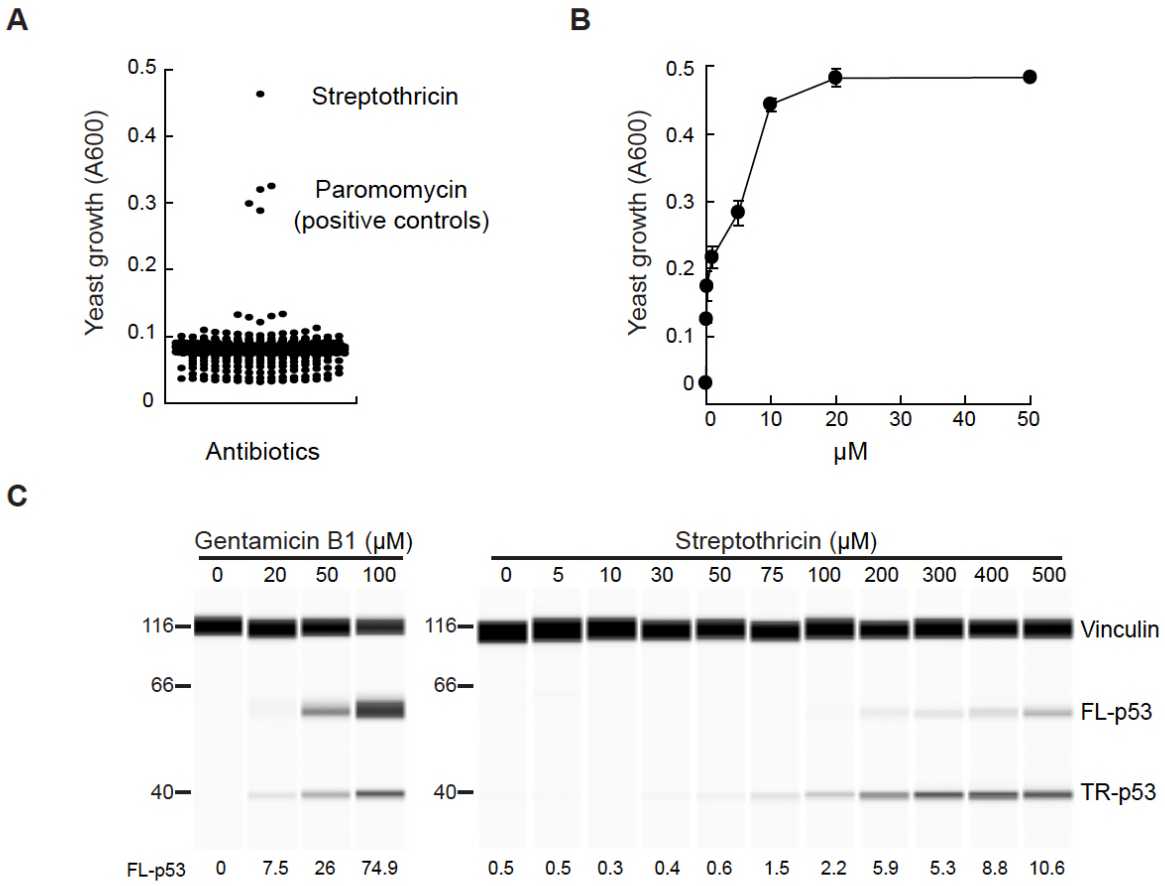

Supplemental Figure 2. Nonsense suppression by streptothricin in yeast and human cells. A. Scatter plot of the nonsense suppression activity of 664 antibiotics in yeast. B. Concentration dependence of nonsense suppression by streptothricin in yeast. C. Concentration dependence of p53 PTC readthrough in HDQ-P1 cells. Formation of full-length p53 (FL-p53) and truncated p53 (TR-p53) was determined by automated capillary electrophoresis western analysis and the results displayed as pseudoblots. FL-p53 and TR-p53 chemiluminescence signal was normalized to that of the protein loading control vinculin and expressed relative to the amount of TR-p53 detected in untreated cells.

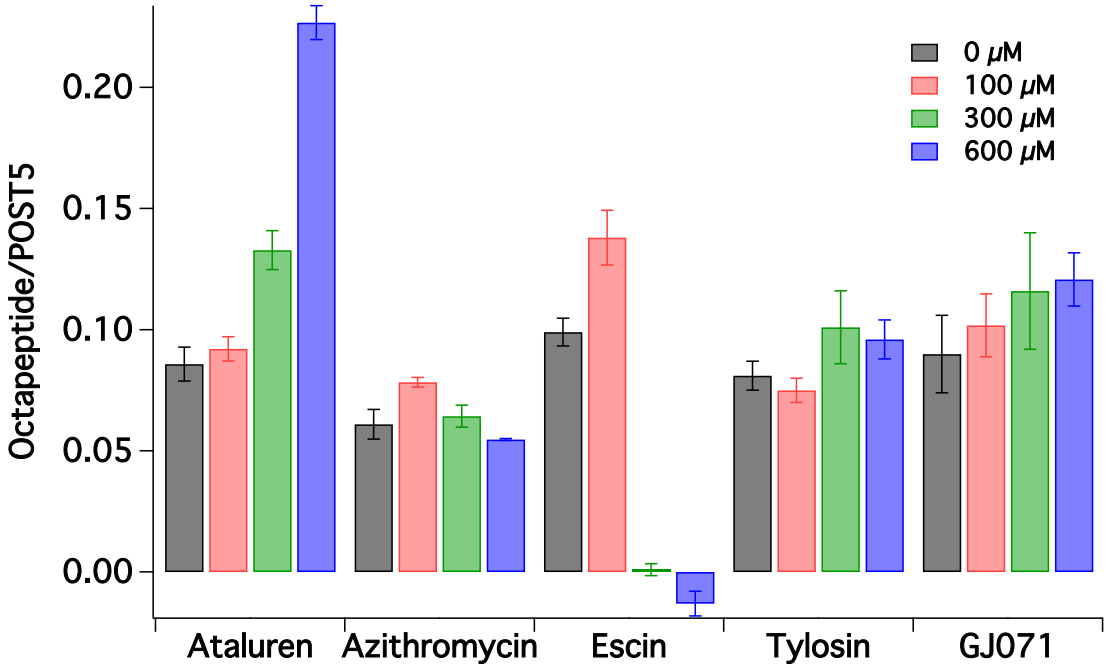

Supplementary Figure 3. Low activity NonSups. With the exception of escin (See Supplementary Figure 4), none of the NonSups in this Figure at 600 μM showed appreciable inhibition of octapeptide formation from pentapeptide by ribosomes programmed with Trp-IRES

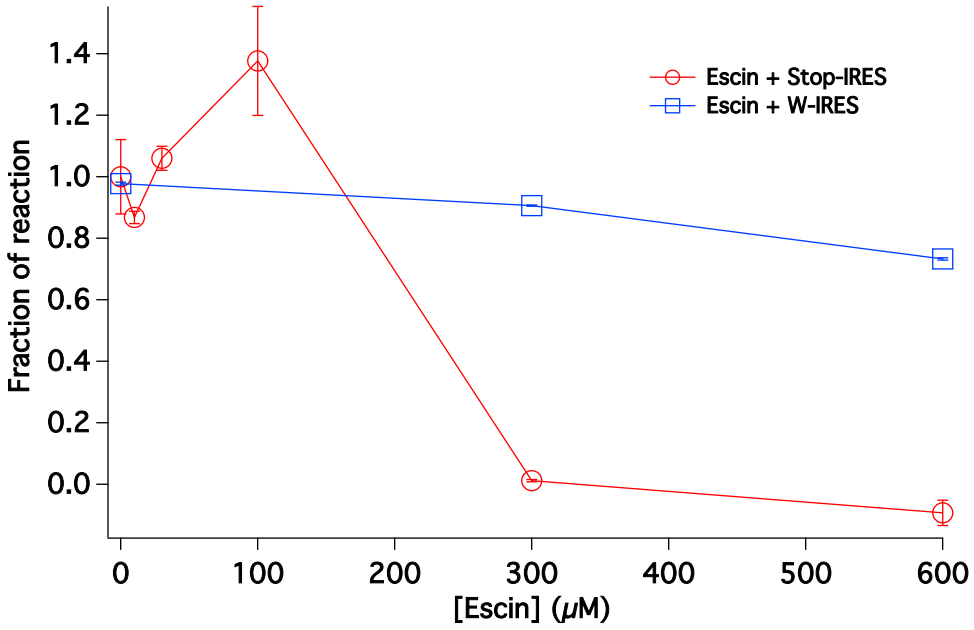

845

846 **Supplementary Figure 4**. High escin concentrations inhibit both basal readthrough (ribosomes

847 programmed with Stop-IRES) and normal octapeptide synthesis (ribosomes programmed with

848 Trp-IRES).

849

850

851

852

853

854

855

856

857

858

859

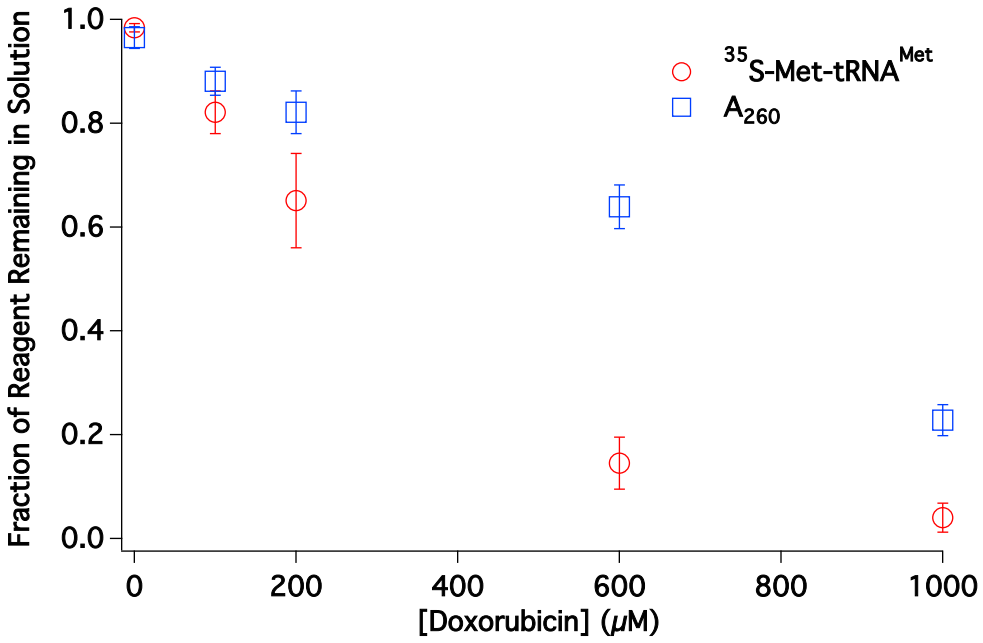

Supplementary Figure 5. High doxorubicin concentrations induce particle formation by both Met-tRNA^{Met} and 80S-IRES complexes.